Separation Science and Technology
Publication details, including instructions for authors and subscription information:
http://www.informaworld.com/smpp/title~content=t713708471

Analysis of Mass Transfer in Unstirred Batch Ultrafiltration: Effect of Variation of Diffusivity in Boundary Layer

Chiranjib Bhattacharjee[a]; Siddhartha Datta[a]
[a] DEPARTMENT OF CHEMICAL ENGINEERING, JADAVPUR UNIVERSITY, CALCUTTA, INDIA

Online publication date: 29 July 1999

To cite this Article Bhattacharjee, Chiranjib and Datta, Siddhartha(1999) 'Analysis of Mass Transfer in Unstirred Batch Ultrafiltration: Effect of Variation of Diffusivity in Boundary Layer', Separation Science and Technology, 34: 11, 2207 — 2221
To link to this Article: DOI: 10.1081/SS-100100766
URL: http://dx.doi.org/10.1081/SS-100100766

SEPARATION SCIENCE AND TECHNOLOGY, **34**(11), pp. 2207–2221, 1999

Analysis of Mass Transfer in Unstirred Batch Ultrafiltration: Effect of Variation of Diffusivity in Boundary Layer

CHIRANJIB BHATTACHARJEE and SIDDHARTHA DATTA*
DEPARTMENT OF CHEMICAL ENGINEERING
JADAVPUR UNIVERSITY
CALCUTTA-700 032, INDIA

ABSTRACT

An unsteady-state mass transfer model has been developed which takes into account the variation of diffusivity with solute concentration in the boundary layer. The main aim of this model is to study the effect of variation of diffusivity on membrane surface concentration as well as on the concentration profile prevailing within the boundary layer. Experimental data generated in this study have been used to validate the model. The resulting complex nonlinear partial differential equation has been solved by a numerical technique. The developed model is also capable of simulating volumetric flux and the permeate volume collected at any time under specified operating conditions. The simulated results show excellent fitting of the present model with variable diffusivity consideration when compared with experimental data. On the other hand, prediction based on constant diffusivity deviates considerably, indicating the importance of consideration of variable diffusivity in unsteady-state batch ultrafiltration.

INTRODUCTION

An important limitation in the performance of pressure-driven membrane processes such as hyperfiltration, ultrafiltration, and microfiltration is concentration polarization (1–3). In general, transmembrane flux is adversely affected by the transient buildup of retained solutes and the resultant presence

* To whom correspondence should be addressed.

of a high solute concentration at the upstream solute–membrane interface. To reduce concentration polarization, modules were developed to allow feed streams to flow tangentially along the membrane surface instead of toward the membrane as in dead-ended or impact flow. This type of crossflow module is usually preferred for industrial use to get high flux. For laboratory purposes, a continuous or batch impact flow module a with flat disc membrane is usually selected. The cell may or may not have the stirring facility, but to study the effect of operating variables, this impact flow configuration is regarded as the best choice (4). Although an unstirred batch cell offers the least flux due to a severe effect of concentration polarization, this cell in many cases has been preferred to study the effect of diffusivity, solution viscosity, as well as different operating parameters on flux and rejection.

Various works have been reported in the literature with unstirred batch cells. Shen and Probstein (5) first attempted the rigorous modeling of unstirred batch cells using constant as well as with variable diffusivity with some approximation to permit solution of the governing partial differential equation. Later, Trettin and Doshi (6) reported an integral method of analysis with the same type of module. The severe effect of concentration polarization as observed in unstirred batch ultrafiltration may ultimately lead to gel formation over the membrane depending upon the type of solute. If the solute does not have a tendency to precipitate over the membrane, the flux will be limited by the osmotic pressure model (7–9), not by the gel polarization model. Severity of concentration polarization may lead to fouling of the membrane, and various research works have also been reported in the literature on the reduction of fouling phenomena (10). The effects of diffusivity on flux and rejection in different types of transport through membranes have been discussed in detail by van den Berg and Smolders (11). Recently, very good work in formulating the concentration polarization phenomenon was reported by Song and Elimelech (12). Their model applies to concentration polarization of nonintersecting particles in a crossflow filtration system. The effects of natural convection instability on membrane performance in dead-end and crossflow ultrafiltration were discussed recently in an interesting manner by Youm et al. (13). Various works regarding the analysis of mass transfer in the boundary layer for batch, continuous, and crossflow ultrafiltration and prediction of flux and rejection have been reported in the literature (14–17). A significant work regarding modeling of concentration polarization and depolarization with high frequency backpulsing was reported by Redkar et al. (18). Recently a unified model for the prediction of flux in stirred and unstirred batch ultrafiltration was also reported (19). An interesting work regarding crossflow filtration of rigid hard spherical solute particles was reported recently by Elimelech and Bhattacharjee (20). The model utilizes the equivalence of hydrodynamic and thermodynamic principles governing equilibrium in a concentration polarization layer.

MARCEL DEKKER, INC.
270 Madison Avenue, New York, New York 10016

Recent literature is very scant regarding the study of diffusional phenomenon in the concentration boundary layer, particularly in the case of a dead-end flat disc module. In unstirred batch ultrafiltration, a step concentration gradient near the membrane surface is expected. Due to this, a rigorous solution of the boundary layer problem with the diffusivity variation properly taken into account is very much needed. The present work deals with unsteady-state batch ultrafiltration with polyethylene glycol (PEG)-6000 as a solute which is reported to be complete miscibility in water. Due to this, the gel polarization model is not applicable for PEG-6000 ultrafiltration; instead, flux limitation will occur due to an increased osmotic pressure difference. A simulation model with a variable diffusivity concept is developed in this study with the main objective of comparing the results with and without variable diffusivity. The developed model is also capable of predicting flux under any operating condition with known membrane hydraulic resistance. Comparison of the results obtained with and without variable diffusivity consideration shows the extent to which this effect is important, particularly in the case of a batch unstirred ultrafiltration cell where a large concentration gradient is observed within the boundary layer. The predicted flux also matches the experimental data generated in this study with a very good fit; the absolute average deviation is $<5\%$.

THEORY

Strictly speaking, the height of liquid over a membrane should decrease with time as the filtration proceeds in the case of unstirred batch ultrafiltration. But since the flux is very low in this case, the content within the cell remains virtually unchanged with time, which results in no significant change in height of the liquid over the membrane. The effect of concentration polarization is most severe in this type of unstirred module because the flux is very low compared to other ultrafiltration module configurations. An unsteady-state mass balance over a differential element of thickness Δx lying at a distance x from a membrane surface gives the following partial differential equation (PDE):

$$\frac{\partial}{\partial x}(Jc) + \frac{\partial}{\partial x}\left(D\frac{\partial c}{\partial x}\right) = \frac{\partial c}{\partial t} \tag{1}$$

For a macromolecular solution the diffusivity can be expressed as a function of solute concentration by the following relation developed by Anderson (21): $D = D_0(1 - \Phi)^{6.5}$, with $\Phi = c/\rho_{PEG} = sc$ where $s = 1/\rho_{PEG}$. After substituting the above equation in Eq. (1), the following PDE can be obtained under the assumption that solution density does not change appreciably, which is true under the present circumstances:

$$J\frac{\partial c}{\partial x} - 6.5sD_0(1 - sc)^{5.5}\left(\frac{\partial c}{\partial x}\right)^2 + D_0(1 - sc)^{6.5}\frac{\partial^2 c}{\partial x^2} = \frac{\partial c}{\partial t} \tag{2}$$

The above equation is to be solved with the following initial and boundary conditions:

$$\begin{aligned} &\text{i)} \quad t = 0,\ c = c_0 \text{ for all } x \\ &\text{ii)} \quad x = 0,\ \frac{\partial c}{\partial x}\bigg|_0 = -\frac{J}{D}(c|_0 - c_\mathrm{p}) \text{ for } t > 0 \\ &\text{iii)} \quad x = H,\ \frac{\partial c}{\partial x} = 0 \text{ for } t \geq 0 \end{aligned} \tag{3}$$

With the introduction of dimensionless variables $\phi = c/c_0$, $\eta = x/H$, and $\psi = D_0 t/H^2$, Eqs. (2) and (3) can be written as

$$\nu_1(\psi)\frac{\partial \phi}{\partial \eta} + \nu_2(\phi)\left(\frac{\partial \phi}{\partial \eta}\right)^2 + \nu_3(\phi)\frac{\partial^2 \phi}{\partial \eta^2} = \frac{\partial \phi}{\partial \psi} \tag{4}$$

with

$$\nu_1(\psi) = \frac{J(t)H}{D_0} \text{ (once } t \text{ is known, } \nu_1 \text{ is also known)}$$

$$\nu_2(\phi) = -6.5sc_0(1 - sc)^{5.5}$$

and

$$\nu_3(\phi) = (1 - sc)^{6.5} \tag{5}$$

which implies that

$$\nu_2 = \partial \nu_3/\partial \phi$$

The above nonlinear PDE is to be solved under the following initial and boundary conditions, written in terms of dimensionless variables:

$$\begin{aligned} &\text{i)} \quad \text{At } \psi = 0,\ \phi = 1 \text{ for all } \eta \\ &\text{ii)} \quad \text{At } \eta = 0,\ \frac{\partial \phi}{\partial \eta} = -\frac{JH}{D_0}\frac{\phi - \phi_\mathrm{p}}{(1 - sc_0\phi)^{6.5}} \\ &\text{iii)} \quad \text{At } \eta = 1,\ \partial\phi/\partial\eta = 0 \text{ for } \psi \geq 0 \end{aligned} \tag{6}$$

Solution Scheme

A numerical technique is used to solve the resulting nonlinear PDE since it does not offer any analytical solution. Among the different numerical techniques, methods based on a finite element are the best from the point of view that the maximum drop in concentration will occur within a very small distance of the membrane surface, although from the theoretical point of view the whole depth of the liquid is taken as the thickness of the concentration bound-

ary layer. The thickness of the finite element must therefore take into account this sharp variation of concentration near the membrane surface with a very small thickness near the membrane which gradually becomes larger far from the membrane. Orthogonal collocation on a finite element (OCFE) has been used to break the PDE into a set of coupled differential equations.

Before applying OCFE, the functions $\nu_2(\phi)$ and $\nu_3(\phi)$ represented by Eq. (5) are unknown when solving for a particular time step. The function $\nu_1(\psi)$ could be known from experimental data after flux (J) is known as a continuous function of time. For this purpose the discrete experimental data collected under specified operating condition in terms of permeate volume (V) versus time (t) are fitted into the following equation:

$$V = \frac{at}{1 + bt} \tag{7}$$

In the case of unstirred batch ultrafiltration, it is expected that the rate of increase of permeate volume, i.e., the volumetric flux, will eventually reduced to zero after a sufficient length of time. Considering the nature of this variation of permeate volume with time, an equation of the form of Eq. (7) has been chosen for the purpose. The parameters of the equation, i.e., a and b, have been fitted by the Lavenberg–Marquardt nonlinear regression technique. The above equation predicts that at a large time, V will remain virtually constant at a/b with negligible flux as is true for unsteady-state batch ultrafiltration. The regression parameters a and b are functions of operating variables (like ΔP and c_b) and different membrane parameters. Once a and b are known, the flux can be calculated by the following equation:

$$J = \frac{1}{A}\frac{dV}{dt} = \frac{a}{A}\frac{1}{(1 + bt)^2} \tag{8}$$

This equation could be substituted into Eq. (5) to determine $\nu_1(\psi)$ as a continuous function of t and hence of ψ. The functions $\nu_2(\phi)$ and $\nu_3(\phi)$, which are also unknown when solving at a particular time $\psi^{(r)}$, are linearized by expansion about the previous time step, $\psi^{(r-1)}$. Thus

$$\nu_2(\phi^{(r)}) = \nu_2(\phi^{(r-1)}) + \left(\frac{\partial \nu_2}{\partial \phi}\right)^{(r-1)} (\phi^{(r)} - \phi^{(r-1)})$$

which can be written as

$$\nu_2(\phi^{(r)}) = Q_1 + Q_2\phi^{(r)} \tag{9}$$

Similarly, $\nu_3(\phi)$ can be linearized and written as follows:

$$\nu_3(\phi^{(r)}) = Q_3 + Q_4\phi^{(r)} \tag{10}$$

The constants Q_1, Q_2, Q_3, and Q_4 are all known at $\psi^{(r)}$ because they involve data at previous time points.

$$\begin{aligned} Q_1 &= Q_4 - Q_2\phi^{(r-1)} \\ Q_2 &= 35.75s^2c_0^2(1 - sc_0\phi^{(r-1)})^{4.5} \\ Q_3 &= \nu_3(\phi^{(r-1)}) - Q_4\phi^{(r-1)} \\ Q_4 &= \nu_2(\phi^{(r-1)}) \end{aligned} \tag{11}$$

So, writing $\nu_1(\psi)$ as Q_5, Eq. (4) can be expressed as follows:

$$Q_5 \frac{\partial\phi}{\partial\eta} + (Q_1 + Q_2\phi)\left(\frac{\partial\phi}{\partial\eta}\right)^2 + (Q_3 + Q_4\phi)\frac{\partial^2\phi}{\partial\eta^2} = \frac{\partial\phi}{\partial\psi} \tag{12}$$

The whole range of integration in the space domain is divided into *NE* number of finite element, each containing *NC* internal collocation points at which the residuals are written. With consideration of the two element boundaries, the total number of points in the space domain is $(NC + 1)NE + 1$, which is written as *NT*. Introducing the local variable *u* in the *k*th finite element where $u = (\eta - \eta^{(k)})/h_k$ with $h_k = \sum_{l=1}^{k-1} h_l$, the PDE (12) can be written as follows by this OCFE technique (22):

$$\begin{aligned} \frac{\partial\phi_i}{\partial\psi} = \frac{Q_5}{h_k}\sum_{J=1}^{NC+2} A_{IJ}\phi_j + (Q_1 + Q_2\phi_i)\left(\frac{1}{h_k}\sum_{J=1}^{NC+2} A_{IJ}\phi_j\right)^2 \\ +(Q_3 + Q_4\phi_i)\,(1/h_k)^2 \sum_{J=1}^{NC+2} B_{IJ}\phi_j \end{aligned} \tag{13}$$

where the global index *i* and local index *I* are related by $i = (k - 1)(NC + 1) + I$ with a similar relation existing between *j* and *J*. The above equation could be written at all internal residual points. The flux continuity at element boundaries requires that

$$\left(\frac{\partial\phi}{\partial\eta}\right)^{\eta_{(\bar{k})}}_{\text{element:}k} = \left(\frac{\partial\phi}{\partial\eta}\right)^{\eta_{(\bar{k})}}_{\text{element:}k+1}$$

which can be written as follows:

$$\frac{1}{h_k}\sum_{J=1}^{NC+2} A_{NC+2,J}\,\phi_{(k-1)(NC+1)+J} = \frac{1}{h_{k+1}}\sum_{J=1}^{NC+2} A_{1,J}\,\phi_{k(NC+1)+J} \tag{14}$$

In this way, $NE - 1$ algebraic equations could be obtained at the internal element boundaries.

Volumetric flux from the osmotic pressure model could be represented by the equation $J = (\Delta P - \Delta\pi)/(\mu R_m)$, which after substitution into the first

boundary condition becomes

$$\frac{1}{h_k}\sum_{J=1}^{NC+2} A_{IJ}\phi_j + \frac{(\Delta P - \Delta\pi)H}{\mu R_m D_0}\frac{\phi_1 - \phi_P}{(1 - sc_0\phi_1)^{6.5}} = 0 \qquad (k = 1) \quad (15)$$

The second boundary condition can be written as

$$\frac{1}{h_k}\sum_{J=1}^{NC+2} A_{IJ}\phi_j = 0 \qquad (k = NE) \quad (16)$$

Equations (14), (15), and (16) comprises $NE + 1$ algebraic equations while Eq. (13) gives a $NE \times NC$ number of differential equation. All these equations can be put into matrix form as follows:

$$\mathbf{CC}\frac{d\boldsymbol{\phi}}{d\psi} = \mathbf{AA}\cdot\boldsymbol{\phi} + \mathbf{F}(\boldsymbol{\phi}) \quad (17)$$

The above equation is to be solved with the initial condition that at $\psi = 0$, $\phi_i = 1$ ($i = 1, \ldots, NT$). **CC** is a diagonal matrix having the following structure:

$CC_{ij} = 0$, if $i \neq j$

$= 1$, if $i = j$ and i corresponds to an internal collocation point

$= 0$, if $i = j$ and i is not an internal collocation point

The function vector has the following structure:

$$F_i = \frac{(\Delta P - \Delta\pi)H}{\mu R_m D_0}\frac{\phi_1 - \phi_p}{(1 - sc_0\phi_1)^{6.5}} \text{ for } i = 1, \text{ i.e., first boundary point}$$

$$= (Q_1 + Q_2\phi_i)\left(\frac{1}{h_k}\sum_{J=1}^{NC+2} A_{IJ}\phi_j\right)^2 + \frac{Q_4\phi_i}{h_k^2}\sum_{J=1}^{NC+2} B_{IJ}\phi_j,$$

for i being an internal collocation point

$= 0$, at element boundary points as well as at the last boundary

An **AA** matrix could be similarly assigned. Equation (17) has been solved by the Crank–Nicholson implicit method to get better accuracy and stability from the "A-stable" method, which can be written after some rearrangement as follows:

$$(\mathbf{CC} - \beta\Delta\psi\mathbf{AA})\boldsymbol{\phi}^{(r)} = [\mathbf{CC} + (1 - \beta)\Delta\psi\mathbf{AA}]\boldsymbol{\phi}^{(r-1)} + (1 - \beta)\Delta\psi\mathbf{F}(\boldsymbol{\phi}^{(r-1)}) + \beta\Delta\psi\mathbf{F}(\boldsymbol{\phi}^{(r)}) \quad (18)$$

where β is a parameter; β = 0.5 is usually chosen. Equation (18) represents a multidimensional nonlinear equation in $\boldsymbol{\phi}^{(r)}$ which is solved by the successive substitution technique. To apply the iterative method, the initial guess chosen was that prevailing at the previous time step, i.e., ${}_{(0)}\boldsymbol{\phi}^{(r)} = \boldsymbol{\phi}^{(r-1)}$. Equation (18) could be written as follows:

$$\mathbf{Z}_{(m)}\boldsymbol{\phi}^{(r)} = {}_{(m-1)}\mathbf{Y} \tag{19}$$

which represents the solution by the successive substitution method, and $\boldsymbol{\phi}^{(r)}$ at the *m*th iteration could be obtained by solving Eq. (19) by Gauss elimination. The procedure may be continued until convergence is reached, and then the evaluation for the next time step could be started. In the above analysis, D_0, the diffusion coefficient at infinite dilution, is obtained for a macromolecular solution by an equation suggested by Sherwood et al. (23). The osmotic pressure is calculated at any desired solute concentration by Flory's equation (24). The different parameters in the equation and the method of evaluation are described elsewhere (25).

Prediction of Flux and Permeate Volume

When the above-mentioned model is used to predict flux, J could not be substituted from Eq. (8) into the PDE. At $t = 0$ (i.e., $\psi = 0$), J is calculated from $J = (\Delta P - \Delta\pi)/(\mu R_m)$ with $\Delta\pi = \pi_0 - \pi_p$, because c_m would be essentially equal to c_0 at the beginning of the ultrafiltration process. The function $\nu_1(\psi)$, i.e., Q_5, has been evaluated at the previous time step, thus when calculating for the first time step the value of Q is known, having been evaluated at $t = 0$. Once the calculation for the first time step is complete, the concentration profile prevailing at t_1 (i.e., ψ_1) is known. This c_m value could be used in the osmotic pressure model to calculate the final value of flux J at t_1. This procedure is followed at all time steps to calculate the flux.

At $t = 0$, the permeate volume (V) is zero. Assuming that flux J would remain constant over Δt (a reasonable assumption owing to the small incremental size), V could be determined from the definition: $V = A\int_0^t J dt$, i.e., $V^{(r)} = V^{(r-1)} + A J^{(r)}\Delta t$, where $V^{(r)}$ is the permeate volume at $t = t_r$. This procedure for the determination of J and V produced excellent results when compared with the experimental data.

EXPERIMENTAL

An unstirred batch cell of 600 mL capacity was used for experimentation. Polyethylene glycol (PEG)-6000 solution was ultrafiltered with an asymmetric cellulose acetate membrane of 5000 MWCO. PEG concentrations of 18, 30, and 40 kg/m^3 with pressure levels of 294.3, 392.4, and 490.5 kPa were used. The total permeate collection was measured at some discrete points

MARCEL DEKKER, INC.
270 Madison Avenue, New York, New York 10016

which were then fitted into Eq. (7) to obtain the values of the parameters a and b by a nonlinear technique. The viscosity of the PEG solution was also calibrated, and it was fitted by an equation of the following form:

$$\mu = (0.80124 + 1.474 \times 10^{-2}\, c + 6.26114 \times 10^{-5}\, c^2 + 4.669 \times 10^{-7}\, c^3)/1000.0 \tag{20}$$

The concentration of PEG-6000 in solution was also determined by the refractive index calibration method.

RESULTS AND DISCUSSION

The objective of the present study was to analyze the boundary layer phenomena as well as to simulate permeate volume and hence flux as a function of time. Furthermore, the membrane used in this study was a high rejecting membrane, with its reflection coefficient value as high as 0.982. When the model was used for analysis, experimental values of flux (J) and permeate concentration (c_p) were used. When V (or J) was simulated, c_p was arbitrarily assigned 5% of c_b, i.e., rejection has been assumed to be 95%. The results in Figs. 3 and 4 were also obtained after assigning a rejection of 95%.

The model developed in this study converges very well in all the time steps. The maximum number of iterations required is 10, but in most cases convergence with a tolerance of 10^{-6} on ϕ_i's is achieved in 5–6 iterations. This suggests a strong convergence characteristic even with the successive substitution technique. The solution scheme has been found to be somewhat sensitive to Δt. The convergence as well as the computed results have been found to be very good for $\Delta t = 0.1$ second to as high as 10 seconds. But after that (i.e., when $\Delta t > 10$ seconds), the model becomes very unstable and in some cases deviates completely from the expected results. Another thing that is very important is the selection of sizes of finite elements. The finite element size near the membrane surface must be very small to account for the strong concentration gradient prevailing in that region, and the sizes can be increased gradually at a distance far away from the membrane. In this study, 15 finite elements were chosen, each with two internal collocation points, thus giving a total of 46 points in the space domain. The development of the concentration profile in the boundary layer with time is shown in Fig. 1. The sharp concentration gradient near the membrane surface is evident from the figure. Initially, the concentration increases very sharply near the membrane surface. After that the rise in concentration becomes slower and finally it tends to the "characteristic concentration" asymptotically, at which the effective driving force becomes zero, i.e., $\Delta\pi \rightarrow \Delta P$. The term "characteristic concentration" is used in conjunction with the osmotic pressure model. Since the gel polarization model is not appropriate for PEG-6000 ultrafiltration, the osmotic pressure model has

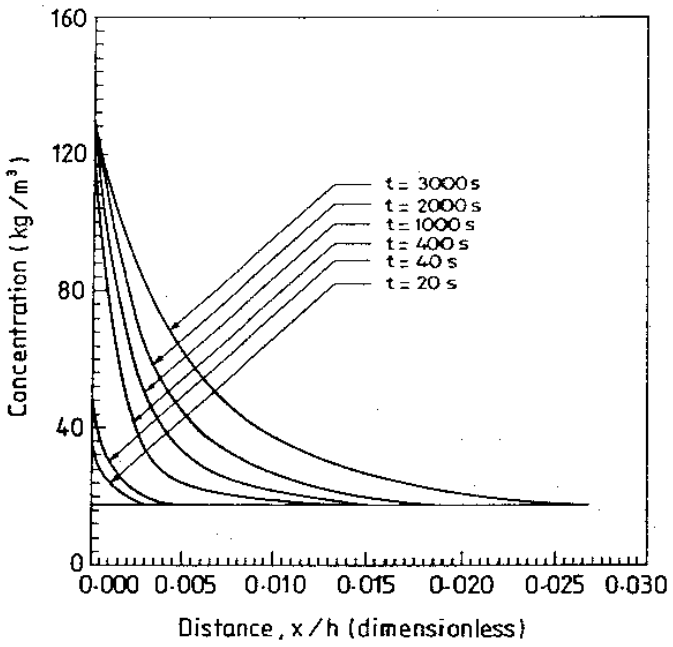

FIG. 1 Development of concentration profile with time under fixed operating conditions (c_b = 18 kg/m^3 and ΔP = 294.3 kPa).

been used in this study to simulate flux, as mentioned earlier. The increased membrane surface concentration resulting from solute rejection causes the osmotic pressure gradient to increase, and there is a particular value of the membrane surface concentration at which the osmotic pressure gradient ($\Delta\pi$) becomes equal to the applied pressure difference (ΔP). At this condition the effective pressure difference, i.e., ($\Delta P - \Delta\pi$), becomes zero, thus giving no flux.

Variations of the membrane surface concentration with pressure and feed concentration are shown in Fig. 2. The results show that as the pressure increases, membrane surface concentration increases as expected. Increased pressure causes more flux, thus more solute is carried to the membrane surface which gives a higher concentration due to continuous accumulation. With an increase in feed concentration, c_m increases quite substantially during the initial period, but in the long run c_m tends to reach the characteristic concentration which is mainly a function of pressure. Thus the difference between c_m values decreases at different c_0 but at the same ΔP at longer times. This figure also shows a comparison between the results obtained with or without consideration of the variable diffusivity. In the model, if s ($= 1/\rho_{PEG}$) is equated to zero, this gives results at constant diffusivity. The membrane surface concentration for the case when c_0 = 18 kg/m^3 and ΔP = 294.3 kPa is around 120 kg/m^3, which, according to the equation used to account for the variation of

diffusivity, gives nearly 52% reduction. This reduced diffusivity near the membrane surface drastically affects the backdiffusional rate by which solute returns to the main bulk of the fluid. Thus, consideration of variable diffusivity increases the membrane surface concentration over that predicted with constant diffusivity. This increased membrane surface concentration causes a larger reverse osmotic pressure gradient, thus reducing the effective driving force. Due to this, the flux as well as the permeate volume are found to be much less than that predicted when constant diffusivity is considered. These findings are shown in Fig. 3 and 4.

The dependence of volumetric flux J with pressure and feed concentration is shown in Fig. 3. The flux increases with an increase in pressure differential, but the increase is not as much as the decrease of flux with feed concentration. With an increase of pressure, c_m also increases, thus raising the value of $\Delta\pi$ which partially offsets the increase in ΔP. Due to this, J does not increase appreciably with a rise in ΔP as expected. An increase in feed concentration also

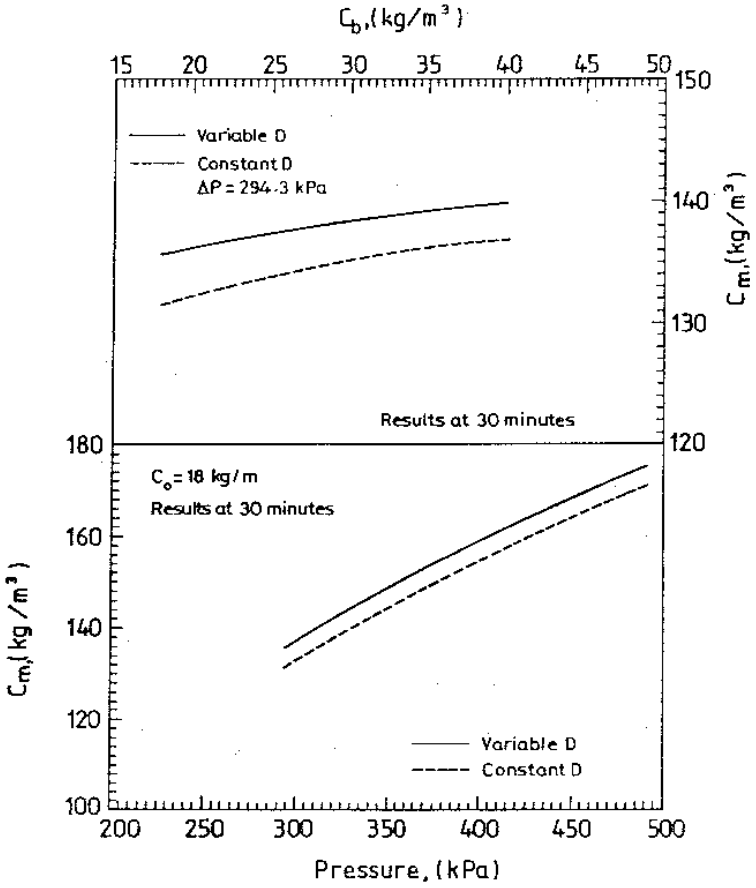

FIG. 2 Membrane surface concentration as a function of pressure differential and bulk concentration, with and without variable diffusivity consideration.

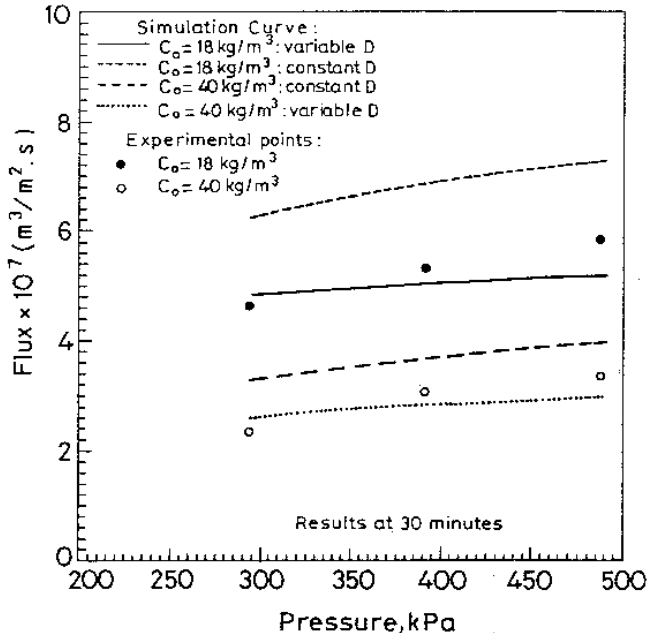

FIG. 3 Volumetric flux as a function of pressure differential and bulk concentration, with and without variable diffusivity consideration.

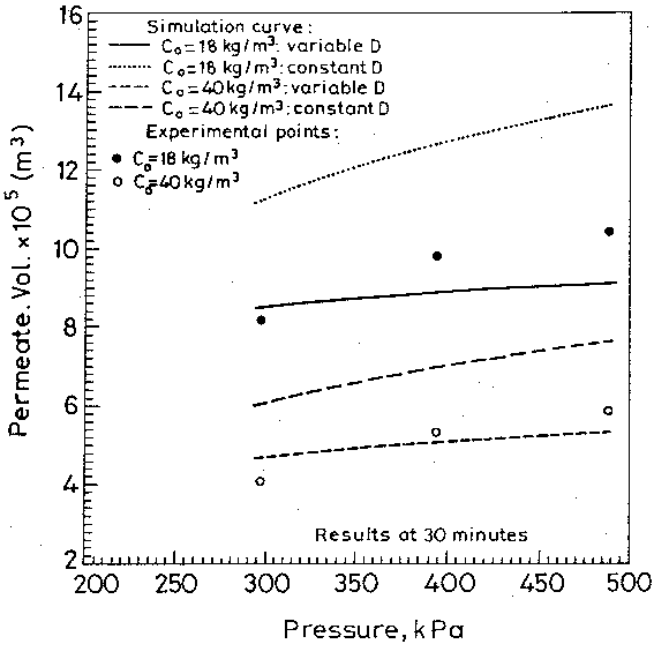

FIG. 4 Permeate volume collection as a function of pressure differential and stirrer speed, with and without variable diffusivity consideration.

MARCEL DEKKER, INC.
270 Madison Avenue, New York, New York 10016

increases the membrane surface concentration marginally, thus reducing the effective pressure differential and flux. There is another and more important reason for flux decline with an increase in c_0, and this is associated with the rise in solution viscosity with concentration. This increased viscosity causes less flux at a higher concentration. Comparison between the results predicted with variable diffusivity and constant diffusivity are shown, and variable diffusivity predicts less flux for the reason explained earlier. The experimental results agree much more with the prediction from variable diffusivity, and this also shows the validity of the present model with variable diffusivity consideration for the prediction of flux.

Variations of permeate volume with ΔP and c_0 are shown in Fig. 4. These results are exactly in accordance with Fig. 3, and the validity of the model with variable diffusivity consideration is obvious from the figure. The absolute average deviation for the prediction of flux and rejection, when computed for all experimental runs under different operating conditions at different times, comes to around 5.2%, which shows the goodness of fit of the present model to the experimental data.

CONCLUSION

A model based on the variable diffusivity concept has been developed in this study to analyze the concentration profile prevailing within the boundary layer, as well as to simulate flux and permeate volume under any operating conditions. The simulated results with variable diffusivity consideration matches very well with the experimental data. The main aim of this study is to assess the importance of change in diffusivity within the concentration boundary layer, and this has been very clearly established.

NOMENCLATURE

A	membrane area (m^2)
$\mathbf{AA}$	a matrix of ($NT \times NT$) order defined in Eq. (17)
$\mathbf{A}$, $\mathbf{B}$	collocation matrix, A_{ij}, B_{ij}: an element in that matrix
a, b	parameters in Eq. (7)
c	concentration (kg/m^3)
c_0	feed (kg/m^3)
c_p	permeate (kg/m^3)
c_m	membrane surface concentration (kg/m^3)
D	diffusivity (m^2/s)
D_0	diffusivity at infinite dilution (m^2/s)
$\mathbf{F}$	function vector defined in Eq. (17)
H	height of liquid over membrane (m)

MARCEL DEKKER, INC.
270 Madison Avenue, New York, New York 10016

h_k	thickness of kth finite element (dimensionless)
J	volumetric flux ($m^3/m^2 \cdot s$)
M	molecular weight (kg/kmol)
MWCO	molecular weight cutoff
P	pressure (N/m^2)
PEG	polyethylene glycol
$Q_1, \ldots, Q_5$	constants defined in Eq. (11)
R_m	membrane hydraulic resistance (m^{-1})
s	constant $= 1/\rho_{PEG}$ (m^3/kg)
t	time (s)
u	local variable defining distance in a finite element
V	permeate volume collection (m^3)
x	distance away from the membrane (m)
$\mathbf{Y}$	vector defined in Eq. (19)
$\mathbf{Z}$	matrix defined in Eq. (19)

Greek Letters

β	parameter defined in Eq. (18)
μ	viscosity (kg/m·s)
ν	function defined in Eq. (5)
π	osmotic pressure (N/m^2)
ρ	density (kg/m^3)
Φ	volume fraction
ϕ	dimensionless concentration $= c/c_0$
η	dimensionless distance $= x/H$
ψ	dimensionless time $= D_0 t/H^2$

Subscripts

i, I	global numbering index and local numbering in a finite element, respectively
j, J	same as i, I
k	kth finite element
m	iteration counter in rth time step

Superscript

r	a counter to account for time step

REFERENCES

1. R. W. Baker and H. Strathman, *J. Appl. Polym. Sci., 14*, 1197 (1970).
2. J. E. Flinn (Ed.), *Membrane Science and Technology*, Plenum, New York, NY, 1970, p. 47.
3. M. C. Porter, *Ind. Eng. Chem., Prod. Des. Dev., 11*, 234 (1972).

MARCEL DEKKER, INC.
270 Madison Avenue, New York, New York 10016

4. W. S. W. Ho and K. K. Sirkar (Eds.), *Membrane Handbook*, Van Nostrand Reinhold, New York, NY, 1992.
5. J. S. Shen and R. F. Probstein, *Ind. Eng. Chem., Fundam., 16*, 459 (1977).
6. D. R. Trettin and M. R. Doshi, *Ibid., 19*, 189 (1980).
7. A. A. Kozinski and E. N. Lightfoot, *AIChE J., 17*, 81 (1971).
8. G. Mitra and J. Landblad, *Sep. Sci. Technol., 13*, 89 (1978).
9. D. R. Trettin and M. R. Dhosi, *ACS Symp. Ser., 154*, 373 (1981).
10. V. G. J. Rodgers and R. E. Sparks, *AIChE J., 37*, 1517 (1991).
11. G. B. van den Berg and C. A. Smolders, *J. Membr. Sci., 73*, 103 (1992).
12. L. Song and M. Elimelech, *J. Chem. Soc., Faraday Trans., 91*(19), 3389 (1995).
13. K. H. Youm, A. G. Fane, and D. E. Wiley, *J. Membr. Sci., 116*, 229 (1996).
14. C. Bhattacharjee and P. K. Bhattacharya, *Ibid., 72*, 137 (1992).
15. C. Bhattacharjee and P. K. Bhattacharya, *Ibid., 82*, 1 (1993).
16. S. Bhattacharjee and P. K. Bhattacharya, *Ibid., 72*, 149 (1992).
17. S. De and P. K. Bhattacharya, *Ibid., 109*, 109 (1996).
18. S. Redkar, V. Kuberkar, and R. H. Davis, *Ibid., 121*, 229 (1996).
19. S. Bhattacharjee, A. Sharma, and P. K. Bhattacharya, *Ibid., 111*, 243 (1996).
20. M. Elimelech and S. Bhattacharjee, *Ibid., 145*, 223 (1998).
21. J. L. Anderson, *Ind. Eng. Chem., Fundam., 12*, 488 (1973).
22. B. A. Finlayson, *Nonlinear Analysis in Chemical Engineering*, McGraw-Hill, New York, NY, 1980.
23. T. K. Sherwood, R. L. Pigford, and C. R. Wilke, *Mass Transfer*, McGraw-Hill, New York, NY, 1975.
24. P. J. Flory, *Principles of Polymer Chemistry*, Cornell University Press, Ithaca, NY, 1953.
25. C. Bhattacharjee and S. Datta, *Sep. Sci. Technol., 31*, 95 (1996).

Received by editor December 3, 1997
Revision received November 1998

PAGE 2222 IS BLANK

MARCEL DEKKER, INC.
270 Madison Avenue, New York, New York 10016

Request Permission or Order Reprints Instantly!